

Accepted Manuscript

Non-linear system identification of a latent heat thermal energy storage system

F. Ghani, R. Waser, T.S. O'Donovan, P. Schuetz, M. Zaglio, J. Wortischek

PII: S1359-4311(17)35028-7

DOI: <https://doi.org/10.1016/j.applthermaleng.2018.02.035>

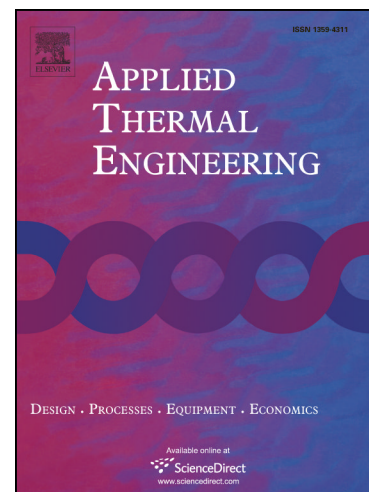
Reference: ATE 11817

To appear in: *Applied Thermal Engineering*

Received Date: 31 July 2017

Revised Date: 30 January 2018

Accepted Date: 10 February 2018



Please cite this article as: F. Ghani, R. Waser, T.S. O'Donovan, P. Schuetz, M. Zaglio, J. Wortischek, Non-linear system identification of a latent heat thermal energy storage system, *Applied Thermal Engineering* (2018), doi: <https://doi.org/10.1016/j.applthermaleng.2018.02.035>

This is a PDF file of an unedited manuscript that has been accepted for publication. As a service to our customers we are providing this early version of the manuscript. The manuscript will undergo copyediting, typesetting, and review of the resulting proof before it is published in its final form. Please note that during the production process errors may be discovered which could affect the content, and all legal disclaimers that apply to the journal pertain.

Non-linear system identification of a latent heat thermal energy storage systemF. Ghani^{1,2}, R. Waser³, T. S. O'Donovan¹, P. Schuetz³, M. Zaglio², and J. Wortischek³¹*Institute of Mechanical, Process, and Energy Engineering, School of Engineering & Physical Sciences, Heriot-Watt University, Edinburgh, United Kingdom*²*Sunamp Ltd., Macmerry, United Kingdom*³*CC Thermal Energy Storage, Lucerne University of Applied Sciences and Arts, Lucerne, Switzerland***Abstract**

Latent heat storage systems utilising phase change materials have potential to offer several advantages over sensible heat storage, including higher energy storage densities and thermal modulation. Despite these advantages, only a few commercialised products incorporating this technology exist due to several engineering challenges. One problem is how to model this technology in a computationally efficient manner which allows simulating this technology with variable heat sources such as solar thermal and heat pump systems and assess their long-term system performance. In this study, the application of a dynamic neural network for this purpose is investigated, where a Layered Digital Dynamic Neural (LDDN) type network is trained using experimental data to approximate the outlet fluid temperature of a latent heat storage system given inlet fluid temperature and mass flow rate.

To acquire the training data necessary for the neural network, an experimental apparatus was designed, built and operated under laboratory conditions. Twenty experiments were conducted to obtain training data where the latent heat storage system was charged to different operating temperatures ranging from 25 to 70 degrees Celsius. The mass flow rate of the heat exchanger fluid flowing through the heat exchanger was also varied: 0.045 and 0.05 kg/s such that the flow of heat exchanger fluid remained turbulent. These data were then presented to the network for training and optimisation of the network architecture using the Bayesian Regularization training algorithm. It was found, that the LDDN type architecture was suitable to characterise the thermal operational behaviour of a latent heat storage system with good accuracy and with little computational effort once trained. Based on an energy analysis, the neural network response predicted the quantity of energy stored and discharged with approximately 5% and 7% accuracy respectively when presented with data not used during the training process. These results indicate that a dynamic neural network may be a computationally efficient method to model the non-linear operational characteristics of a latent heat storage system. It may therefore be implemented within a simulation environment such as TRNSYS or Simulink.

Keywords: Dynamic neural network; latent heat storage; phase change material; modelling; thermal characterisation

1.0 Introduction

According to the results presented in the latest REN21 report [1], the addition of renewable power capacity has overtaken fossil fuel powered sources. Due to the intermittency typically experienced by renewable energy sources such as solar and wind, energy storage technologies are essential components for these systems to address the mismatch between the supply of energy and user demand. This issue is particularly relevant to solar energy systems, where solar radiation is converted to electricity and heat via photovoltaic and solar thermal technologies respectively. An additional need for storage arises when there is a disparity between the rate of energy supplied from a renewable energy source, and the rate at which it is required at time of use is considered. Frequently, applications require energy transfer rates during operation far higher than the rate at which it is collected; this is the case for air-sourced heat pumps and solar thermal systems for domestic hot water applications. In Europe, it has been estimated that approximately 1.4 million GWh/year could be saved and some 400 million tons of CO₂ emissions avoided in the building and industrial sectors with increased penetration of thermal energy storage [2]. The focus of this work therefore is on thermal storage systems for solar thermal systems to address the above-mentioned issues.

Currently, commercialised thermal energy storage technologies may be largely split into two categories based on the dominant mode of heat transfer: sensible and latent heat types. For sensible

heat storage, storage is obtained proportionately with material temperature while in a single state of phase. Here, water tanks are frequently used based on its high specific heat capacity, availability, low cost, and non-toxicity. These systems are heavily used for low-to-medium temperature solar thermal systems where water is stored at circa 60°C to meet domestic hot water needs.

Latent heat storage however leverages the heat of fusion/vaporisation phenomena experienced during the change in phase of a material. Thermal energy storage via latent heat offer several advantages over sensible heat storage including significantly higher energy storage density and consequently a reduction in overall system volume as well as exhibiting near isothermal operation during the charge and discharge cycles [3]. For latent heat storage, the storage capacity Q_s may be determined using Eq. (1) [4].

$$Q_s = \int_{T_1}^{T_2} mc_p(T)dT + m \cdot f \cdot \Delta q \quad (1)$$

Where T_1 and T_2 are the initial and final temperatures in K respectively, m is the mass of the PCM medium in kg, c_p is the specific heat value for the phase change material (PCM) in J/kg K, f is the melt fraction, and Δq is the latent heat of fusion in J/kg.

The phase change process may take place via solid-solid, liquid-gas, and solid-liquid phase transitions. For the solid-solid mode, heat is stored by transition between distinct kinds of crystallisation forms. Incredibly high latent heat values are achieved via the liquid-gas transition, however, the large volumetric change during this process poses a significant engineering challenge. The solid-liquid phase transition however does not experience as significant a change in volume and has therefore been investigated in many studies. Applications include the implementation of PCM into building materials [5, 6], cold storage for cooling plants [7], low temperature (45-60°C) for heating plants [8], and hot water storage for solar cooling and heating (<80°C) [9, 10].

Phase change materials may be classified as either organic, inorganic, or eutectic with the first two types most frequently used. Organic PCMs such as paraffin waxes involve the crystallisation of chain n-alkenes where a large quantity of latent heat is released. Alternative organic PCMs include esters, fatty acids, alcohols, and glycols [11], however, these materials typically suffer low thermal conductivities and instability at high temperatures [12, 13].

Inorganic salt hydrate PCMs possess a number of advantages including: limited supercooling, negligible change in melting enthalpy with cycling, and improved thermal conductivity (over organic PCMs) [14]. The heat exchanger has been commercialised and is currently being manufactured with a PCM with a melting temperature of circa 58°C, making it suitable for domestic hot water applications. The technology may be integrated within several system types such as:

1. Photovoltaic systems with enhanced self-consumption. Here, electricity provided by the photovoltaic panels is converted to heat by an electric cartridge heater, heating water which is then used to charge the PCM store. These systems are useful to increase the consumption of any clean energy produced by a photovoltaic array when it is not beneficial to the household to export electricity back to the grid.
2. Solar thermal systems. Solar thermal collectors are capable of efficiently converting solar radiation into heat via an absorption process. Heat collected from these panels may then be used to directly charge a PCM filled latent heat storage system.
3. Heat pump systems. Air and ground sourced heat pumps, where heat from ambient and ground respectively is transferred to a higher temperature sink via mechanical work require coupling with thermal energy storage. Heat rejected by the condenser from such a system may be used to charge the PCM.

Regardless of the system design and the heat source used to charge the latent heat storage system, modelling and simulation is necessary to optimise its integration into the overall system. This is particularly true when coupling the storage system with a variable heat source such as a solar thermal collector as the performance is not only dependent on its installed climate and collector performance specifications, but also the behaviour of the entire system. For this purpose, computer simulation tools are often employed such as Polysun (Vela Solaris, Switzerland), T*Sol (Valentin Software GmbH, Germany), and TRNSYS (TESS, USA). Currently, these popular software packages possess extensive libraries for sensible heat storage but not for latent heat storage. Due to the phase change

phenomenon, this is not a simple problem to address. In this study, we examine the suitability of training a recurrent type neural network to model the non-linear dynamic behaviour of a heat exchanger filled with the sodium acetate based PCM developed by Sunamp Ltd. In the next section, a brief review is made of the numerical approach that has traditionally been applied. An introduction to the recurrent neural networks is then made followed by the research method, results, and conclusions.

1.1 Numerical modelling approach

The mathematical formulation of phase transition from liquid to solid or vice versa, known as the Stefan problem, consists of two coupled partial differential equations (i.e. one for each phase), as well as an energy equation applied at the phase boundary [15]. Analytic solutions can be found for simple 1-D cases [16] but numerical schemes are required to solve more complex problems, which commonly appear in practical engineering applications. The numerical approaches can be divided into deforming and grid fixed grid schemes. The deforming grid schemes require complicated mathematic operations to track the phase interface which leads to high computational costs [17]. Fixed schemes, however, do not require an explicit tracking of the phase interface [18]. A widely used fixed grid scheme is the so-called enthalpy method [19-22]. The two partial differential equations of the Stefan problem are reduced to a single equation of enthalpy which can be written as:

$$\rho \frac{\delta h}{\delta t} = \nabla \cdot (\lambda \nabla T) \quad (2)$$

where ρ is the temperature dependent density and λ the thermal conductivity of the material. The specific enthalpy h consists of the sensible heat and the latent heat Δq released or absorbed during phase change and can be described as:

$$h = \int_{T_{ref}}^T c_p dT + f \Delta q \quad (3)$$

c_p represents the specific heat capacity of the material and T_{ref} is an arbitrary reference temperature. The phase indicator f represents the liquid fraction within a control volume and depends on the temperature of the material. In literature, many authors use following definition [23]:

$$f = \begin{cases} 0 & \text{if } T < T_{PC,s} \text{ (solid)} \\ \frac{T - T_{PC,s}}{T_{PC,l} - T_{PC,s}} & \text{if } T_{PC,l} < T < T_{PC,s} \text{ (mushy)} \\ 1 & \text{if } T > T_{PC,l} \text{ (liquid)} \end{cases} \quad (4)$$

In the equations above, $T_{PC,s}$ describes the temperature at which the material starts to solidify. Furthermore, $T_{PC,l}$ is the melting temperature. Accordingly, the phase change takes place within a temperature range, the so called mushy zone. The mushy-zone avoids sharp discontinuities which may lead to numerical instabilities[24]. It is worth mentioning that the enthalpy method, as described above, does not account for natural convection since no mass and momentum conservation is described. However, methods to include natural convection, as an adaption of the thermal conductivity of the material in the liquid phase[25, 26] exist but will not be discussed in more detail hereafter.

The enthalpy method is applicable for complex geometries since it can be discretised using finite volume as well as finite element methods. In the field of latent heat storage, a considerable number of investigations based on the enthalpy method have been investigated elsewhere [27-30] [13] [14] [15] [16]. Numerical schemes are a suitable method to design and optimise heat exchange concepts in latent heat storage systems, however, they are not the method of choice regarding annual system simulations due to their high computational burden. In this study, an empirical approach based on the application of a dynamic neural network based on their computational efficiency allowing long term system level performance calculations to be calculated.

1.2 The LDDN type neural network

Neural networks may generally be largely classified as either static or dynamic. Static networks based on the standard feed forward multi-layer perceptron architecture are extensively used for pattern and

function approximations where the output is calculated directly from the input through feed forward connections. The output from a dynamic network however, is dependent on both the current input and history of the input sequence. Consequently, dynamic networks possess memory, allowing these architectures to learn time series patterns for a range of applications including the prediction in financial markets, speech recognition, and phase detection in power systems [31]. The current research investigates the suitability of applying a dynamic neural network, particularly the Layered Digital Dynamic Network (LDDN) architecture, to perform non-linear system identification on a latent heat storage device.

Each layer in the LDDN is made up of a set of weight matrices based on connections from other layers or from external inputs, associated weight function rule base used to combine the weight matrix with its input, and associated tapped delay line. Additionally, a bias vector, net input function rule is used to combine outputs of the various weight functions with the bias to produce the net input, and a transfer function.

The dynamic neural network is trained using a gradient based algorithm like that used by a standard multi-layer perceptron (MLP) network employing the backpropagation procedure. Due to the more complex impact of the weights within a dynamic network, where the weights have both direct impact on the output from a neuron at the current time step and the indirect effect the weights may also have on inputs from other layers, more complex dynamic backpropagation learning algorithms are required; these are computationally demanding and therefore more time is needed to solve.

In a previous study, a feed-forward back-propagation artificial neural network was trained for carrying out heat transfer analysis on the phase change process in a finned-tube type latent heat storage device [32]. In this study, a neural network with four inputs parameters was created; heat transfer area, Reynolds number, inlet temperature of heat transfer fluid, and time. The network was designed with a single output, the stored thermal energy by the heat exchanger. It was found in their study that the response from the neural network better matched the experimental data than a numerical method. It was finally concluded in their work that the neural network approach to modelling latent and sensible heat storage systems was a promising approach.

The procedure for creating a neural network for a specific application involves:

1. Collecting the experimental data from the system.
2. Pre-processing of experimental data.
3. Defining the appropriate number of hidden layers.
4. Specifying the optimal number of hidden layer neurons where a balance between accuracy and ability to generalise from inputs not contained within the training set is struck.
5. Using the correct combination of transfer functions such as the sigmoid, hyperbolic tangent, or pure linear functions.
6. Train the network using a suitable training algorithm with a suitable early stop criterion.
7. Testing the network with data not used during the training process and evaluate its robustness.

The proceeding section will address each of these points specifically for the development of a neural network for non-linear system identification of a latent heat storage system.

2.0 Research Method

The method applied to create a dynamic neural network to dynamically model the charge and discharge process of a latent heat storage system is discussed in this section. The objective of the neural network model developed in this study is to approximate the outlet fluid temperature from the heat exchanger given two inputs; i) inlet fluid temperature (T_1), and ii) the inlet mass flow rate in kg/s (m) as shown in Figure 1. These two parameters were taken as network inputs as the key physical inputs into the system which can be easily measured. Ambient temperature was not considered due to the use of vacuum insulation panels and their excellent ability to retard heat loss. Training will be based on both charge and discharge phases of the energy storage device.

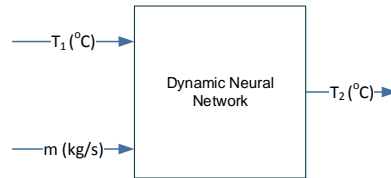


Figure 1 Input/output schematic of model developed in this study. Where T_1 is the inlet fluid temperature, m is the mass flow rate of fluid entering the PCM filled heat exchanger, and T_2 is the outlet fluid temperature from the heat exchanger.

The latent heat storage device investigated in this work is a commercialised product manufactured by Sunamp Limited in the United Kingdom. The system comprises of a dense tube-and-fin type heat exchanger made up of aluminium fins and a copper tube encased in a polymer housing. This heat exchanger, shown in Figure 2, is filled with a patented inorganic phase change material based on a sodium acetate trihydrate formula during the production process while in liquid form. The heat exchanger consists of a single copper tube and therefore has only one inlet and one outlet port. Based on this design the heat exchanger cannot be simultaneously charged and discharged. Properties of the phase change material are provided in Table 1.

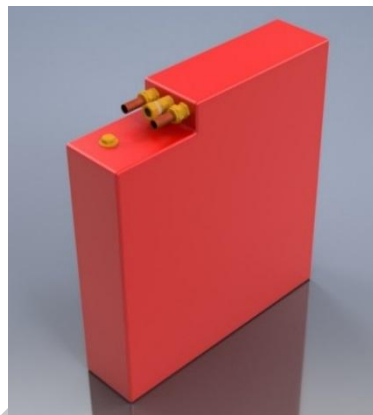


Figure 2 CAD diagram of the Sunamp latent heat storage device.

Table 1 Material properties of the phase change material used in the latent heat TES for this study.

Manufacturer	Sunamp Ltd (United Kingdom) Patent Number: WO2014195691
Composition	Sodium acetate trihydrate + additives
Melting temperature	58°C
Density	1.28 kg/litre (liquid 75°C)
	1.44 kg/litre (solid 20°C)
Heat of fusion	226 kJ/kg
Specific heat capacity	2.8 kJ/kg/K (Solid 20°C)
	3.5 kJ/kg/K (liquid 75°C)
Maximum Temp	80°C

A single Sunamp heat exchanger (see Figure 3) has approximately 2.5 kWh capacity, sufficient to heat close to 50L of water by 40 degrees Celsius. In this study, two Sunamp heat exchangers were hydraulically coupled in a series scheme to provide a total of 5 kWh of storage. Here, the outlet from the first heat exchanger is the input to the second heat exchanger.

To train the neural network, extensive experimental data is required. For this, an indoor experimental apparatus was designed and built with a data acquisition system for logging the experimental data of interest. Details of this experimental apparatus are provided in the proceeding section.

2.1 Acquisition of neural network training data

A schematic of the experimental apparatus used to collect the data for training the neural network is shown in Figure 3. The experiment consists of two fluid loops:

1. Loop 1 is used to provide heat to charge the latent heat storage devices via a 2kW electric cartridge heating element. This loop contains a 5L header tank containing a working fluid (water), heating element, pump, and instrumentation for temperature and flow measurement. Water is circulated around this closed loop via P01 (see Figure 3) and its flow rate is measured using a turbine type brass flowmeter (see component 'FM-01').
2. Loop 2 is used to thermally charge and discharge the latent heat exchangers (see components labelled 'RC1' and 'RC2' in Figure 3). Heat is transferred from the plate heat exchanger to the water circulating inside this loop during the charging process. Heat collected by the circulating water is then transferred to the PCM contained within the latent heat storage devices. Conversely during the discharge process, low temperature mains water is circulated through this loop where it is then heated by the PCM.

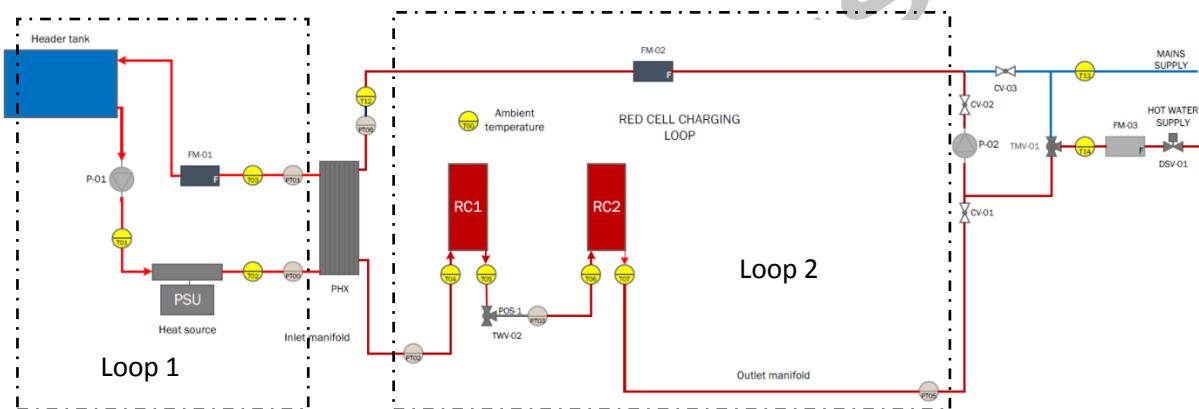


Figure 3 Schematic of the experimental apparatus used for this study with location of all thermocouples (TXX), pressure sensors (PTXX), flow meters (FMXX), control valves (CVXX), pumps (PXX), and power supply unit (PSU).

During the charging process, heat is transferred from the heated fluid circulating in loop 1 to the working fluid circulating in loop 2 via a SWEP brazed plate heat exchanger (model B5THx10, see component 'PHX' in Figure 3). The heated fluid exiting the plate heat exchanger enters the first storage device ('RC1') where heat is then rejected to the PCM during the charging phase. Fluid exiting RC1 then enters the second storage device ('RC2') to similarly charge the PCM contained within. Due to this series connected fluid arrangement, RC1 will be both charged and discharged first.

Referring to Figure 3, thermocouples and flow meters were installed throughout the system to measure fluid temperatures and the flow rates at which the streams are being circulated in both loops. All temperature measurements were made using mineral insulated k-type thermocouples with a probe diameter of 3 mm. The thermocouples were installed such that the probe tip was immersed and in direct thermal contact with the fluid at point of measurement. The flowmeters were brass body turbine types (Model FTB370, Omega Instruments UK), were installed to measure the flow rates within loops 1 and 2. Each flowmeter produced a fixed number of pulses per litre which were counted using a National Instruments digital input/output module with counter measurement (model number NI-9401). Thermocouples T-04 and T-07 measured the inlet and outlet fluid temperatures while FM-02 was used to measure the mass flow rate during the charge and discharge process.

The two identical Grundfos solar pumps installed accepted a pulse width modulated signal (PWM) for flow modulation. A 500Hz PWM signal was generated using the NI-9401 Digital Input / Output module to control pumps P-01 and P-02 (see Figure 3). All instruments including thermocouples, flow meters and PWM signals were programmatically read and controlled using bespoke software developed using the programme LabVIEW.

The programme was also responsible for controlling the charge and discharge timing of the experiments conducted. Here, a simple strategy was employed where the series connected red cells would be continually charged until the outlet fluid temperature measured using T-07 (see Figure 3) reached a specified value (T_{charge}). Once this temperature was reached and the charging phase completed, the electric cartridge heating element and all pumps were switched off and the solenoid valve DSV-01 (see Figure 3) was opened; this allowed mains water to circulate through loop 2, discharging heat from the heat batteries. The discharge process continued until the temperature of the fluid measured using T-07 fell below a specified value ($T_{discharge}$). During the charge and discharge process, the data required to train the neural network was logged at a frequency of 1 Hz.

To ensure the neural network was sufficiently trained, a series of twenty experiments were conducted where the latent heat storage system was charged to a range of temperatures for two mass flow rate values, and then discharged. Details of the experiments conducted are provided in Table 2. For all experiments conducted, the power of the electric cartridge heating element was fixed at 2000W. The discharge flow rate was fixed at 0.12 kg/s as indicated in Table 2. The increase in mass flow rate is achieved via mains pressure water being circulated through the heat exchangers during the discharge phase.

Table 2 Outline of the experiments carried out to collect the neural network training data.

Experiment	T_{charge}	$T_{discharge}$	m_{charge} (kg/s)	$m_{discharge}$ (kg/s)
1	70	15	0.05	0.12
2	65	15	0.05	0.12
3	60	15	0.05	0.12
4	55	15	0.05	0.12
5	50	15	0.05	0.12
6	45	15	0.05	0.12
7	40	15	0.05	0.12
8	35	15	0.05	0.12
9	30	15	0.05	0.12
10	25	15	0.05	0.12
11	70	15	0.045	0.12
12	65	15	0.045	0.12
13	60	15	0.045	0.12
14	55	15	0.045	0.12
15	50	15	0.045	0.12
16	45	15	0.045	0.12
17	40	15	0.045	0.12
18	35	15	0.045	0.12
19	30	15	0.045	0.12
20	25	15	0.045	0.12

Data collected from the experiments outlined in Table 2 were pre-processed using a moving average filter prior to network training. The proceeding section will discuss the architecture of the neural network trained using this data.

2.2 Design and validation of neural network

Using the neural network design tool in Matlab, the training data collected as described in the previous section was used to design the neural network. The single training sequence consisted of twenty charge/discharge cycles (see Table 2 for details). Twenty experiments were conducted to

initially collect data for a finite range of charge/discharge cycles which covered an extensive range of the typical operation by a thermal energy storage system. A greater number of experiments would provide more data for neural network training but will result in significantly greater computational effort and training time. For this investigation into the feasibility of dynamic neural networks to model a latent heat TES, twenty experiments was deemed to be sufficient. The entire training sequence consisted of 21,863-time steps. The number of experiments may need to be increased if during the testing phase the performance of the neural network was not adequate.

This sequence was partitioned into two groups, one used for training the network where the Bayesian Regularization learning algorithm [33] was applied to adjust the synaptic weights of the neural network, and the second set for testing the network where a mean square error (MSE) approach was used to evaluate the performance of the network. The data was split 90% for training and 10% for testing.

Many parameters may be adjusted to optimise the architecture of a neural network for a specific application. These include:

1. The learning algorithm applied
2. The number of hidden layers
3. The number of hidden layer neurons in each hidden layer
4. The activation function used by each layer's neurons
5. The number of input and feedback delays

Architecture and elements of a typical LDDN network is shown in Figure 4.

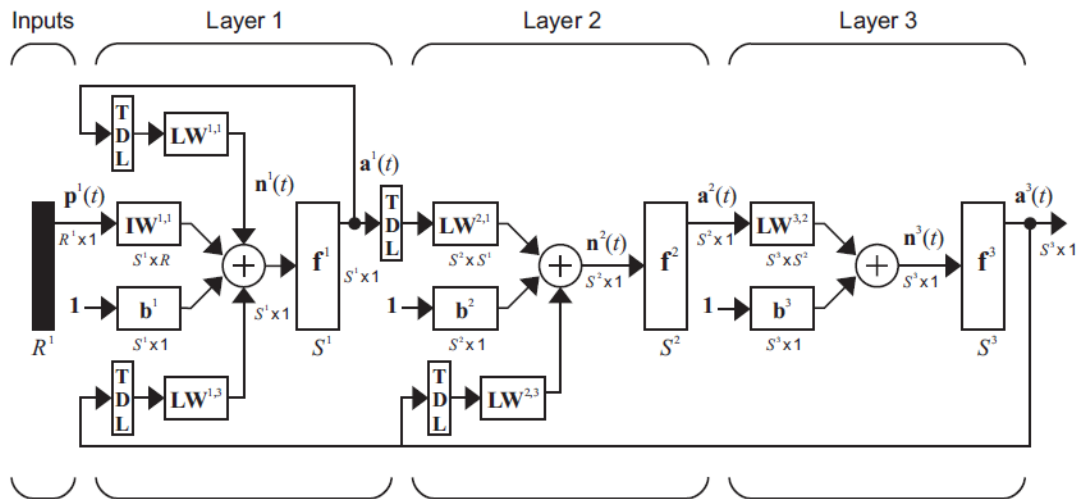


Figure 4 Schematic of the Layered Digital Dynamic Network (LDDN). TDL = tapped delay line, LW = hidden layer weights, IW = weights in the input layer, b = bias unit, and f = transfer function.

Several training algorithms may be used for training dynamic neural networks including the Levenberg-Marquardt (LM), Bayesian regularization (BR), and scaled conjugate gradient (SCG) types. The LM method is based on a second order approach which bypasses the need to compute the Hessian matrix using a sum of squares approach. The LM method progresses towards the solution using a hybrid gradient/Newton method striking a balance between robustness and speed. Although memory intensive, this method is popular due to its faster training time. It was found, however, that Bayesian Regularization backpropagation algorithm gave the best results for this specific application. Here, the Levenberg-Marquardt procedure is used to update the weights and biases throughout the network during the training phase while aiming to produce a network that generalises well by minimising a combination of squared errors and weights, and yielding the correct combination. A comparison between the two methods carried out by authors demonstrated that only a minor difference in the final performance would result from training the neural network with these two methods with the BR method resulting in a slightly higher performing network.

The ideal number of hidden layers (see Figure 4) found in this work was three, with each layer consisting of eleven hidden layer neurons in each layer giving a total of 518 weight elements. This neural network architecture, was found via a trial and error approach where the mean square error value was used as the key performance metric. It was sought during this process that a MSE value of 0.01 was obtained from the testing phase. This value represented a value low enough to achieve the desired accuracy, while being large enough not to lead to overtraining.

Each of the hidden and output layer neurons were activated using the hyperbolic tangent sigmoid function in all layers. The hyperbolic tangent function, see Eq. (5), is a rescaling of the logistic sigmoid function such that its asymptotes are located at $y=1$ and -1 . A time step delay of seven for both the inputs and feedback was found to be suitable for this problem.

$$\tanh(t) = \frac{e^t - e^{-t}}{e^t + e^{-t}} \quad (5)$$

3.0 Results and Discussion

Using the experimental apparatus described in the previous section, the latent heat storage system was charged to varying temperatures as specified in Table 2. Figure 5 below plots the inlet and outlet fluid temperatures for a single charge/discharge process. Here the storage device is heated until a temperature of 70 degrees Celsius is obtained during the charging phase. Inspecting this figure, we observe three regions as indicated. In the first region, sensible heat transfer prior to reaching the melting temperature of the phase change material is observed as the temperature rises linearly with time (heat source is constant at 2000W for all experiments). In the next stage, latent heat transfer is observed once the inlet fluid temperature has reached and exceeded the melting temperature of the PCM (i.e. $T = 58^\circ\text{C}$) as indicated by the plateau (with a shallow gradient). Once the PCM is melted and in liquid form, heat transfer is via sensible heating occurs once again as we observe a linear temperature rise with time. Following the charge phase, cold mains water is then circulated through the heat exchanger resulting in energy discharge from the PCM. During the discharge phase, we observe a different profile as the PCM is now undergoing a solidification process.

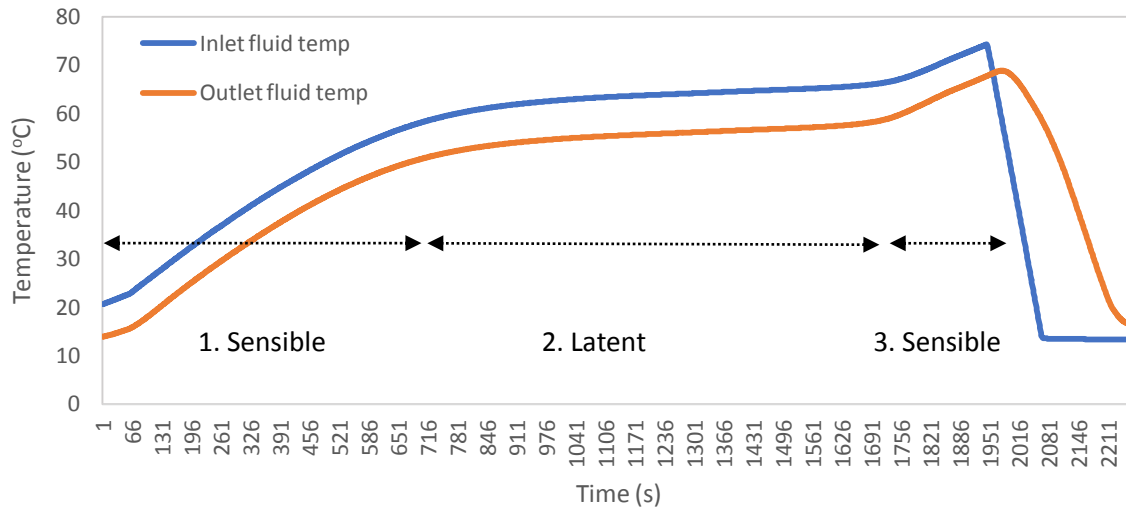


Figure 5 Experimental data collected for a single charge and discharge cycle for the latent heat storage system tested.

To first evaluate the network, the response from the neural network was compared to the experimental data used during the training phase which was collected from the twenty experiments outlined in Table 2. The neural network response, with an architecture described in the previous section, is shown in Figure 6 alongside the experimental data. Here, the experimental outlet fluid temperature data is presented alongside the neural network response. Examining Figure 6, we can see qualitatively that there is good agreement between the response of the neural network and the experimental data. The error may be quantified via a root mean square error (RMSE) analysis approach calculated using Eq. (6).

$$RMSE = \sqrt{\frac{1}{n} \sum_{i=1}^n (T_{EXP,i} - T_{ANN,i})^2} \quad (6)$$

Applying Eq. (6), the RMSE value for neural network was found to be 0.009°C.

The root mean square error value obtained and the results presented in Figure 6 demonstrate that a dynamic neural network can carry out the non-linear system identification of the latent heat storage device under study in this work. One of the primary reasons for implementing the neural network solution is to reduce computational time. Using the tic/toc command in Matlab, the time required to generate the output temperatures used for Figure 6, consisting of twenty charge/discharge cycles was 1.7 seconds. These calculations were performed using a laptop with Intel(R) Core(TM) i5-6440HQ processor clocked at 2.60GHz.

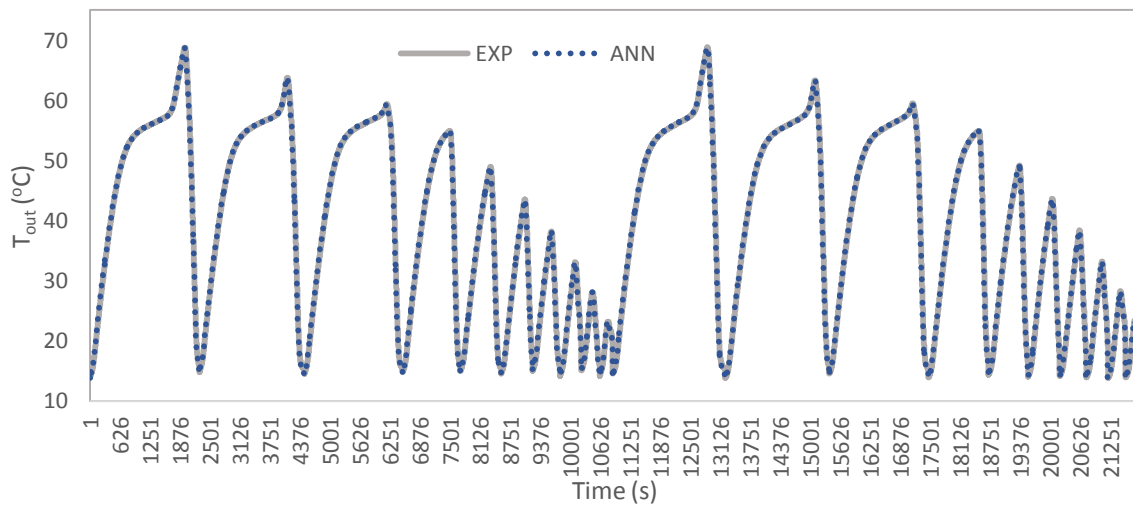


Figure 6 Comparing the response from the dynamic neural network (dashed series) against the experimental data (solid series) during the training process.

The ability for the network to generalise is an important aspect of the network. Here, data not used to train the network but within the domain of the training data, is presented to the network and its response evaluated. An experiment was conducted on the indoor experimental apparatus where the latent heat storage system was charged to 68°C with a mass flow rate of 0.05 kg/s. Looking again at Table 2, we can see that the network was trained specifically at T = 70 and 65°C at this mass flow rate value. The results are presented in Figure 7. Inspecting this figure, we can see that the neural network response (dashed data set) matches the experimental response with a good overall fit. The response from the neural network is excellent for the charging process where we observe a small disparity between its response with the experimental data. During the discharge process, however, we see that there is some mismatch between the data sets. This difference between the neural network response and the charge/discharge experimental data is attributed to the different physical mechanisms taking place during operation. During the charging process, the PCM is slowly melting while during the discharge process the PCM is undergoing rapid solidification process. To enhance the accuracy of the discharge process, further training is needed to improve the networks response.

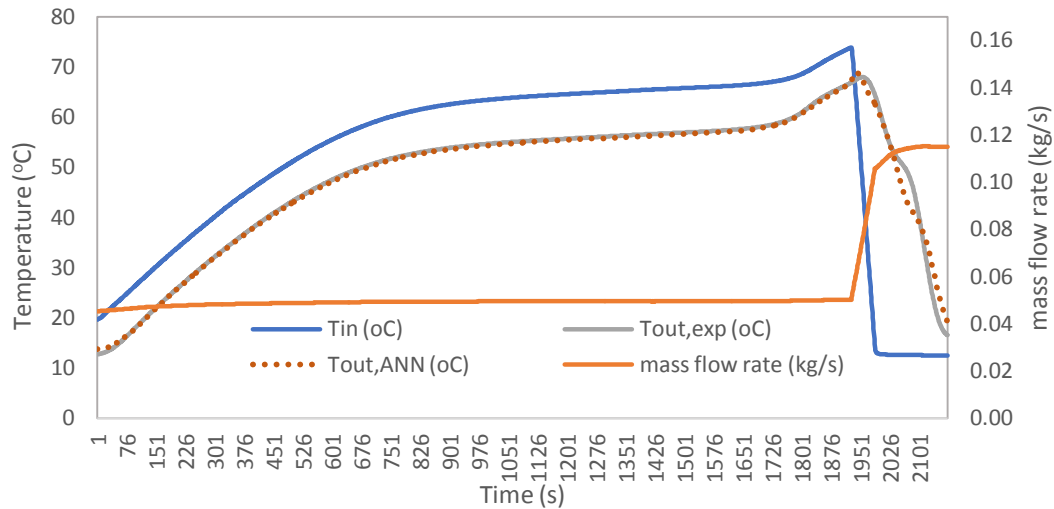


Figure 7 Comparing the neural network response against the experimental data for a charge temperature of 68°C.

A more extensive data set was collected from the experimental test rig where the latent heat storage system was charged to eight different temperatures from $T = 68$ to 42 degrees Celsius. The neural network response and experimental data sets are shown in Figure 8. Like the results presented in Figure 7, the network's response for the charging process is very good, with some disparity emerging for the discharge process but with an overall good fit. Using the tic/toc command in Matlab, the results presented in Figure 8 took 1.36 seconds to generate.

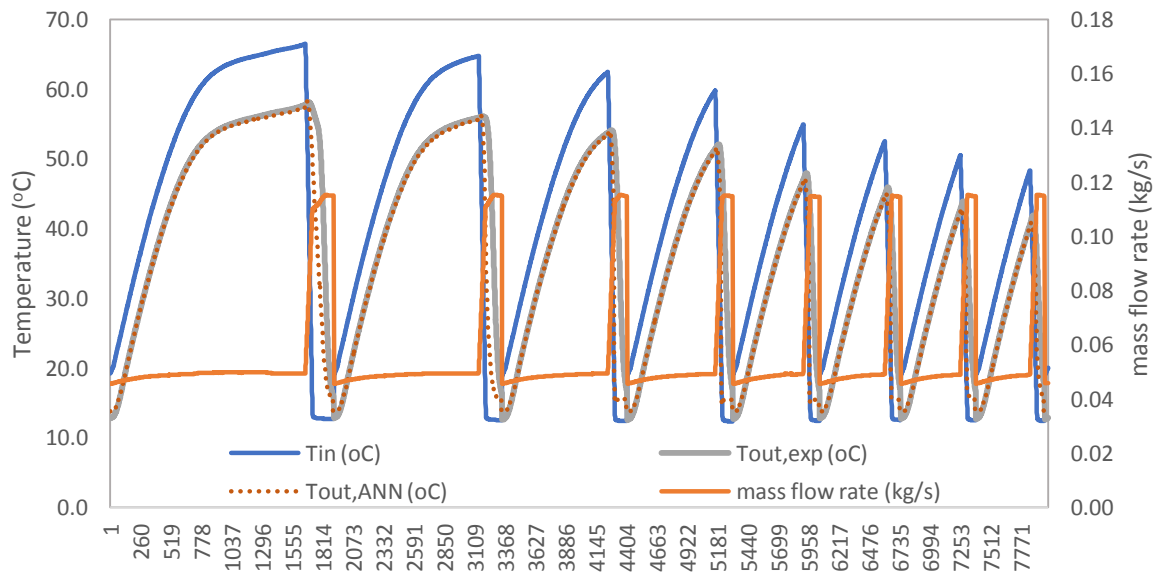


Figure 8 Response of neural network for test data set where data not used to train the network is presented for testing.

The coefficient of determination values for the different training and testing sets were calculated to be 0.999 and 0.889 respectively in this study. Although a reduction in accuracy was experienced in the testing phase, the high R^2 value suggest the network can learn the relationship between the input and output variables.

The neural network model may be used to carry out an energy analysis to quantify the amount of energy stored and discharged from the latent heat storage device. The power transmitted during storage and discharge is calculated using Eq. (7) and Eq. (8).

$$\dot{Q}_{stored} = \dot{m}C_p(T_{in} - T_{out}) \quad (7)$$

$$\dot{Q}_{discharged} = \dot{m}C_p(T_{out} - T_{in}) \quad (8)$$

Using Eq. (7) and Eq. (8), we can determine the amount of energy stored and discharged from the heat batteries from both the experimental and neural network data and compared. Tabulated results are provided in Table 3. Data set 1 and Data set 2 represent the training and test data sets corresponding to the data plotted in Figures 6 and 8. All numerical values provided in Table 3 are provided in kilowatt hours (kWh). For Data set 1, the neural network response is excellent for both charge and discharges cycles with error less than 0.1% based on a comparison of energy values. For the test data set, where data not used for training the network is presented, the storage and discharges errors increase to 5.1 and 7.1% respectively. Although there is a significant increase in error over the training data set, these values are adequate for time-efficient approximations. Training the network with more extensive data sets would see these values decrease. Further training will require the collection of more experimental data where a larger number of operating parameters are varied.

Table 3 Energy analysis results where the neural network values for storage and discharge cycles are compared to the experimental data. All numerical values are provided in kilowatt hours (kWh).

Data set	Description	Q_{stored} (Exp)	Q_{stored} (ANN)	$Q_{discharged}$ (Exp)	$Q_{discharged}$ (ANN)
1	Training data set	8.1317	8.1245	7.0421	7.0493
2	Test data set	6.6351	6.9737	6.0342	5.6026

4.0 Conclusions

In this study, a dynamic neural network has been developed to empirically model the thermal characteristics of a latent heat storage system. The latent heat TES investigated in this work consisted of an inorganic salt PCM.

Training data for the neural network was compiled from a total of twenty experiments conducted using an indoor experimental apparatus. It was found that the neural network could accurately map the input/output relationship with a mean square error value of less than 0.01 obtained during the training phase.

Further testing was conducted where experimental data were collected at operating conditions different to the training set using the experimental apparatus. Although the neural network had not previously seen this data, a coefficient of determination of approximately 0.9 was obtained demonstrating it could model the charging process with acceptable accuracy. Although excellent accuracy was obtained during the charging phase of operation where the PCM is slowly melted, some disparity emerged during the discharge process due to the rapid solidification process. Based on an energy analysis, it was found that the error between the neural network and experimental data for the charge and discharge phases were approximately 5.1 and 7.1% respectively.

The results from this study demonstrate the suitability of training a dynamic neural network to model the non-linear operation of a heat exchanger filled with phase change material for energy storage and discharge. It offers a computationally efficient method to characterise their performance where charge/discharge cycles can be calculated in just a few seconds using a standard desktop personal computer. It may therefore be used for long term energy using software packages such as TRNSYS (via a Matlab call function). The limitation of this approach however, is the experimental data required for training the network. Extensive data must be collected where the latent heat storage system is operated under different operating conditions. In comparison to training static type neural networks, dynamic neural network training is a computationally time-consuming process.

References

- [1] R. Secretariat, Renewables 2017 global status report, REN21, Paris, Tech. Rep, (2017).
- [2] I. IRENA, The energy technology systems analysis programme (ETSAP): technology brief E17, in, 2013.

- [3] L.F. Cabeza, *Advances in thermal energy storage systems: Methods and applications*, Elsevier, 2014.
- [4] G.A. Lane, *Solar heat storage: latent heat materials*, (1983).
- [5] A.M. Khudhair, M.M. Farid, A review on energy conservation in building applications with thermal storage by latent heat using phase change materials, *Energy conversion and management*, 45 (2004) 263-275.
- [6] L.F. Cabeza, A. Castell, C.d. Barreneche, A. De Gracia, A. Fernández, Materials used as PCM in thermal energy storage in buildings: a review, *Renewable and Sustainable Energy Reviews*, 15 (2011) 1675-1695.
- [7] B. He, F. Setterwall, Technical grade paraffin waxes as phase change materials for cool thermal storage and cool storage systems capital cost estimation, *Energy conversion and management*, 43 (2002) 1709-1723.
- [8] M.M. Farid, A.M. Khudhair, S.A.K. Razack, S. Al-Hallaj, A review on phase change energy storage: materials and applications, *Energy conversion and management*, 45 (2004) 1597-1615.
- [9] F. Bruno, *Using Phase Change Materials (PDMs) for Space Heating and Cooling in Buildings*, in, Citeseer, 2004.
- [10] M. Mazman, L.F. Cabeza, H. Mehling, M. Nogues, H. Evliya, H.Ö. Paksoy, Utilization of phase change materials in solar domestic hot water systems, *Renewable Energy*, 34 (2009) 1639-1643.
- [11] A. Abhat, D. Heine, M. Heinisch, N. Malatidis, G. Neuer, Development of a modular heat exchanger with integrated latent heat energy store, Final Report, Dec. 1979 Institut fuer Kemtechnik und Energiewandlung eV, Stuttgart (Germany, FR). (1981).
- [12] I. Sarbu, C. Sebarchievici, Chapter 4 - Thermal Energy Storage, in: *Solar Heating and Cooling Systems*, Academic Press, 2017, pp. 99-138.
- [13] A. Stamatiou, M. Obermeyer, L.J. Fischer, P. Schuetz, J. Worlitschek, Investigation of unbranched, saturated, carboxylic esters as phase change materials, *Renewable Energy*, 108 (2017) 401-409.
- [14] F. Bruno, M. Belusko, M. Liu, N.H.S. Tay, 9 - Using solid-liquid phase change materials (PCMs) in thermal energy storage systems A2 - Cabeza, Luisa F, in: *Advances in Thermal Energy Storage Systems*, Woodhead Publishing, 2015, pp. 201-246.
- [15] J. Stefan, Über die Theorie der Eisbildung, insbesondere über die Eisbildung im Polarmeere, *Annalen der Physik*, 278 (1891) 269-286.
- [16] C. Hsieh, Exact solutions of Stefan problems for a heat front moving at constant velocity in a quasi-steady state, *International journal of heat and mass transfer*, 38 (1995) 71-79.
- [17] S. Wang, A. Faghri, T.L. Bergman, A comprehensive numerical model for melting with natural convection, *International journal of heat and mass transfer*, 53 (2010) 1986-2000.
- [18] Z. Ma, Y. Zhang, Solid velocity correction schemes for a temperature transforming model for convection phase change, *International Journal of Numerical Methods for Heat & Fluid Flow*, 16 (2006) 204-225.
- [19] Z. Younsi, H. Naji, A numerical investigation of melting phase change process via the enthalpy-porosity approach: Application to hydrated salts, *International Communications in Heat and Mass Transfer*, 86 (2017) 12-24.
- [20] V.R. Voller, C. Prakash, A fixed grid numerical modelling methodology for convection-diffusion mushy region phase-change problems, *International journal of heat and mass transfer*, 30 (1987) 1709-1719.
- [21] V. Voller, M. Cross, Accurate solutions of moving boundary problems using the enthalpy method, *International journal of heat and mass transfer*, 24 (1981) 545-556.
- [22] V. Voller, M. Cross, Estimating the solidification/melting times of cylindrically symmetric regions, *International journal of heat and mass transfer*, 24 (1981) 1457-1462.
- [23] F. Rösler, D. Brüggemann, Shell-and-tube type latent heat thermal energy storage: numerical analysis and comparison with experiments, *Heat and mass transfer*, 47 (2011) 1027.
- [24] D.W. Hahn, M.N. Özişik, *Heat Conduction Fundamentals*, Heat Conduction, Third Edition, (2012) 1-39.
- [25] H. Pointner, A. De Gracia, J. Vogel, N. Tay, M. Liu, M. Johnson, L.F. Cabeza, Computational efficiency in numerical modeling of high temperature latent heat storage: Comparison of selected software tools based on experimental data, *Applied Energy*, 161 (2016) 337-348.
- [26] M.M. Farid, R.M. Husian, An electrical storage heater using the phase-change method of heat storage, *Energy conversion and management*, 30 (1990) 219-230.
- [27] C. Zauner, F. Hengstberger, M. Etzel, D. Lager, R. Hofmann, H. Walter, Experimental characterization and simulation of a fin-tube latent heat storage using high density polyethylene as PCM, *Applied Energy*, 179 (2016) 237-246.

- [28] S. Wu, G. Fang, X. Liu, Dynamic discharging characteristics simulation on solar heat storage system with spherical capsules using paraffin as heat storage material, *Renewable Energy*, 36 (2011) 1190-1195.
- [29] B.N. Sponagle, D. Groulx, Numerical study of temperature control in tablet computers using phase change material thermal energy storage, in: *Fourth Int. Forum Heat Transf. IFHT*, 2016, pp. 1-6.
- [30] M. Jradi, M. Gillott, S. Riffat, Simulation of the transient behaviour of encapsulated organic and inorganic phase change materials for low-temperature energy storage, *Applied thermal engineering*, 59 (2013) 211-222.
- [31] L. Medsker, L.C. Jain, *Recurrent neural networks: design and applications*, CRC press, 1999.
- [32] K. Ermis, A. Ereğ, I. Dincer, Heat transfer analysis of phase change process in a finned-tube thermal energy storage system using artificial neural network, *International journal of heat and mass transfer*, 50 (2007) 3163-3175.
- [33] D.J. MacKay, Bayesian interpolation, *Neural computation*, 4 (1992) 415-447.

Highlights:

- A computationally efficient method to characterise a latent heat store is proposed
- Method based on a dynamic neural network
- Experimental data collected to compile training data
- Neural network tested against experimental data for testing
- Results demonstrate that a dynamic neural network is suitable for this application

ACCEPTED MANUSCRIPT